

Enhanced Next-to-Leading-Order Corrections to Weak Annihilation B -Meson Decays

Cai-Dian Lü^{a,b}*, Yue-Long Shen^c†, Chao Wang^d‡ and Yu-Ming Wang^e§

^a Institute of High Energy Physics, CAS, P.O. Box 918(4), Beijing 100049, China

^b School of Physics, University of Chinese Academy of Sciences, Beijing 100049, China

^c School of Physics and Optoelectronic Engineering, Ocean University of China,
Songling Road 238, Qingdao, Shandong 266100, P.R. China

^d Department of Mathematics and Physics, Huaiyin Institute of Technology,
Meicheng East Road 1, Huaian, Jiangsu 223200, P.R. China

^e School of Physics, Nankai University, Weijin Road 94, Tianjin 300071, P.R. China

(Dated: February 17, 2022)

We accomplish the analytical computation of the pure weak annihilation non-leptonic B -meson decay amplitudes at leading power in the heavy quark expansion. The novel observation regarding such fundamental hadronic quantities is that adding the missing hard-collinear contribution on top of the hard gluon exchange effect eliminates rapidity divergences entering the convolution integrals of factorization formulae. Subsequently we identify the perturbative enhancement mechanism due to the penguin contractions of the current-current operators from the weak effective Hamiltonian, which yields the significant impacts on the CP violating observables.

INTRODUCTION

It is generally accepted that the exclusive two-body charmless bottom-meson decays are of fundamental importance for advancing our understanding towards diverse facets of the strong interaction dynamics governing the flavour-changing heavy-quark decay processes and for exploring the peculiar implications of the Cabibbo-Kobayashi-Maskawa (CKM) mechanism for CP violation in electroweak interactions. The primary challenge of predicting such hadronic B -meson decay observables consists in constructing a field-theoretic framework to disentangle the calculable perturbative QCD fluctuations from the non-perturbative soft and collinear physics systematically. In this respect, the QCD factorization formalism based upon expansions in the small parameter Λ_{QCD}/m_b [1–6] has proven to provide the precise prescriptions for evaluating the appeared non-leptonic matrix elements of the effective weak Hamiltonian operators. However, the long-standing obstacle to improve the factorization calculations of the two-body B -meson decay amplitudes arises from the disturbing end-point divergences in the convolution integrals describing the power-suppressed but phenomenologically pronounced weak annihilation corrections. In particular, the inadequacy of achieving the factorization-compatible regularization of the annihilation amplitudes apparently does not allow to provide quantitative predictions for the annihilation-dominated decay processes.

Additionally, the abiding lack of higher-order perturbative corrections to the weak annihilation topologies prevents us from obtaining reliable estimates of the strong-phase sensitive quantities (for instance, the direct CP asymmetry) due to a variety of potential enhancements, which do not manifest themselves at leading-order (LO) in the strong coupling. The process-independent

parametrizations for logarithmically and linearly divergent integrals in the basic building blocks for the exclusive hadronic $\bar{B}_q \rightarrow PP$, $\bar{B}_q \rightarrow PV$ and $\bar{B}_q \rightarrow VV$ (with $q = d, s$) decay amplitudes [7–10] (see also [11–13] and references therein) introduce further assumption for the current QCD factorization predictions, especially with the finite bottom-quark mass in practice, which has been examined exploratorily by employing the data-driven strategy [14–19]. The striking importance of the weak annihilation mechanism in investigating the non-leptonic B -meson decay amplitudes also motivated the interesting dynamical anatomy [20–22] on the basis of distinct QCD techniques (see [23–31] for an alternative treatment taking into account the non-vanishing transverse momenta of the active partons). As a consequence, accomplishing the systematic computation of the weak annihilation topologies with the non-trivial strong phases will be of the top priority for developing the conceptual framework of the charmless two-body $\bar{B}_q \rightarrow M_1 M_2$ decays and for better confronting the anticipated precision measurements of a large number of CP violating observables at the Belle II experiment [32].

In order to probe factorization properties of the weak annihilation contributions immaculately, we report on a novel observation of the hard-collinear gluon exchange (the short-distance configuration with the invariant mass of $\mathcal{O}(\sqrt{m_b \Lambda_{\text{QCD}}})$) in regularizing the unwanted rapidity divergences analytically, which has been unfortunately neglected in all previous calculations of the two-body hadronic B -meson decays, by concentrating on the pure annihilation channels such as $\bar{B}_s \rightarrow \pi\pi$ and $\bar{B}_d \rightarrow \phi\phi$. The significance of this essential insight for consolidating the theory foundation of QCD factorization in B -meson decaying into two light mesons will be further strengthened by inspecting a sample set of the next-to-leading order (NLO) Feynman diagrams, which are enhanced

by the large Wilson coefficients and/or the multiplication CKM factors numerically and are promising to yield the sizeable strong phases. General implications of the improved formalism on the accessible decay observables will be then discussed with the acceptable models for the leading-twist light-cone distribution amplitudes of both the bottom meson and the final-state hadrons.

GENERAL ANALYSIS

We start by setting up our notation of the effective weak Hamiltonian of the non-leptonic $\Delta B = 1$ transitions in the Standard Model (SM)

$$\begin{aligned} \mathcal{H}_{\text{eff}} = & \frac{4 G_F}{\sqrt{2}} \sum_{p=u,c} V_{pb} V_{pq}^* \left[C_1(\nu) P_1^p(\nu) + C_2(\nu) P_2^p(\nu) \right. \\ & + \sum_{i=3}^6 C_i(\nu) P_i(\nu) + \sum_{i=3}^6 C_{iQ}(\nu) P_{iQ}(\nu) \\ & \left. + C_{7\gamma}(\nu) P_{7\gamma}(\nu) + C_{8g}(\nu) P_{8g}(\nu) \right], \end{aligned} \quad (1)$$

where we adopt the effective operator basis introduced in [33–37] enabling the disappearance of Dirac traces with γ_5 . The renormalized Wilson coefficients $C_i(\nu)$ with $\nu \sim \mathcal{O}(m_b)$ will be evaluated for our purpose in the next-to-leading-logarithmic (NLL) approximation in the Chetyrkin-Misiak-Münz basis [34].

It proves convenient to cast the exclusive transition amplitude governing the weak-annihilation bottom-meson decay in the form

$$\begin{aligned} \bar{\mathcal{A}}(\bar{B}_q \rightarrow M_1 M_2) = & -\langle M_1(p_1) M_2(p_2) | \mathcal{H}_{\text{eff}} | \bar{B}_q(p_B) \rangle \\ = & \mp i \frac{4 G_F}{\sqrt{2}} f_B f_{M_1} f_{M_2} \sum_{p=u,c} V_{pb} V_{pq}^* (\pi \alpha_s) \frac{C_F}{N_c^2} \\ & \times \left[\mathcal{T}^{p,(0)} + \left(\frac{\alpha_s}{4\pi} \right) \mathcal{T}^{p,(1)} + \mathcal{O}(\alpha_s^2) \right], \end{aligned} \quad (2)$$

where the upper sign in (2) applies for $M_1 M_2 = PP, V_L V_L$, while the lower sign when $M_1 M_2 = PV, VP$. We leave out the discussion on final states consisting of two transversely polarized vector mesons, bearing in mind that the resulting helicity amplitudes are power-suppressed when compared with the counterpart longitudinal polarization amplitude [9]. The appearing LO quantities $\mathcal{T}^{p,(0)}$ can be determined by evaluating the first two Feynman diagrams in Figure 1, where we also display the relevant diagrams generating the dynamically enhanced contributions to the NLO pieces $\mathcal{T}^{p,(1)}$. It remains important to remark that the additional LO annihilation diagrams with the gluon radiation off the final-state partons (not included in Figure 1) lead to the vanishing effects for the pure annihilation channels in the limit of symmetric distribution amplitudes and under the assumption of the SU(3) flavour symmetry as noted in [2].

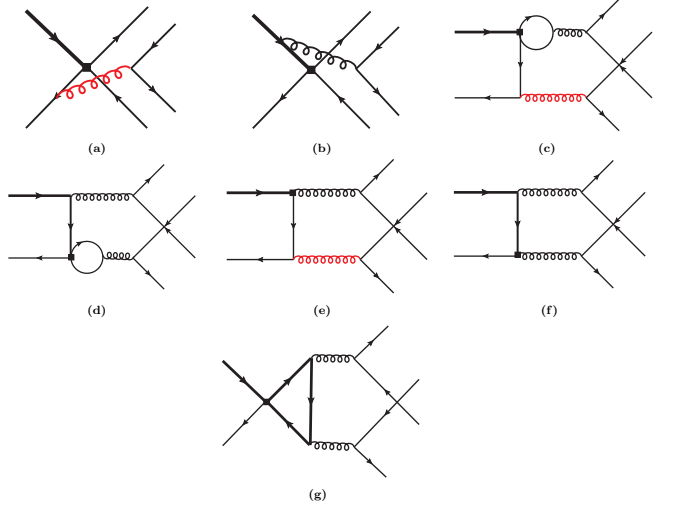


FIG. 1. Sample Feynman diagrams for the weak annihilation $\bar{B}_q \rightarrow M_1 M_2$ decays at LO and NLO. The gluons marked with red colour can carry either the hard or hard-collinear momentum, while the remaining gluons can only possess the hard momentum. Symmetric diagrams that follow from (c)–(g) by exchanging the two off-shell gluons are not displayed.

Taking advantage of the flavour-decomposition strategy [8] allows us to write down

$$\begin{aligned} \mathcal{T}^{p,(0)} = & \delta_{pu} \mathcal{C}_{M_1 M_2}^{(1)} \mathcal{B}_1(M_1 M_2) + \mathcal{C}_{M_1 M_2}^{p,(4)} \mathcal{B}_4(M_1 M_2) \\ & + \mathcal{C}_{M_1 M_2}^{p,(4,\text{EW})} \mathcal{B}_{4,\text{EW}}(M_1 M_2). \end{aligned} \quad (3)$$

The prefactors $\mathcal{C}_{M_1 M_2}^{(p), (i, (\text{EW}))}$ collect the Clebsch-Gordan coefficients from the flavour structures of the \bar{B}_q -meson as well as the final-state mesons and they further absorb the electric-charge coefficients from P_{iQ} . The phenomenologically dominating effects of $\mathcal{T}^{p,(1)}$ can be categorized in terms of their topological structures

$$\begin{aligned} \mathcal{T}^{p,(1)} \supset & \sum_{i=1}^6 C_i \mathcal{P}_i^{p,(1)}(M_1 M_2) + C_8^{\text{eff}} \mathcal{P}_{8g}^{(1)}(M_1 M_2) \\ & + \sum_{i=1}^6 C_i \mathcal{I}_i^{p,(1)}(M_1 M_2), \end{aligned} \quad (4)$$

with $C_8^{\text{eff}} = C_{8g} + C_3 - C_4/6 + 20C_5 - 10C_6/3$ [38]. We will dedicate the next section to the analytical computation of the flavour amplitudes $\mathcal{B}_{i,(\text{EW})}$ and the NLO building blocks $\mathcal{P}_{1\dots 6,8g}^{p,(1)}$ and $\mathcal{I}_i^{p,(1)}$ within QCD factorization.

QCD FACTORIZATION FOR DECAY AMPLITUDES

Establishing the factorization formulae for the hadronic quantities $\mathcal{B}_{i,(\text{EW})}$ can be customarily achieved by investigating the appropriate partonic amplitudes of

the tree diagrams (a) and (b) in Figure 1 in the leading-twist approximation. The yielding contribution due to the gluon emission from the bottom quark (i.e., the LO diagram (b)) has been demonstrated to be calculable self-consistently at twist-two order [2, 39]. We are then led to atomize the infrared behaviour of the effective matrix element represented by the first diagram in Figure 1 (with an insertion of P_2^u for the illustration purpose)

$$\langle P_2^u \rangle_{(a)}^{(0)} = (\pi \alpha_s) \frac{C_F}{N_c^2} \int_0^\infty d\omega \int_0^1 dx \int_0^1 dy \\ \text{Tr} \left\{ \mathcal{M}^B(v, \omega) \left[\gamma_{\perp\nu} \left(\not{p}_1 + \not{q}_2 - \not{k} \right) \gamma_\mu (1 - \gamma_5) \right] \right. \\ \left. \mathcal{M}^{M_1}(p, y) [\gamma_\perp^\nu] \mathcal{M}^{M_2}(q, x) [\gamma^\mu (1 - \gamma_5)] \right\} \\ \times \frac{1}{[(p_1 + q_2 - k)^2 + i\epsilon][(p_1 + q_2)^2 + i\epsilon]}, \quad (5)$$

where the explicit expressions of the momentum-space projection operators \mathcal{M}^B , \mathcal{M}^{M_1} and \mathcal{M}^{M_2} have been derived in [7, 9, 40, 41] (see [42] for the original discussion on B -meson distribution amplitudes in heavy quark effective theory (HQET) and [43] for an alternative construction of the on-shell light-cone projectors). Here we have assigned the four-momenta $p_{1,2}$ ($q_{1,2}$) to the quark and antiquark in the energetic meson M_1 (M_2). The dimensionless variable y (x) refers to the momentum fraction carried by the quark field in the composite M_1 (M_2) system in the (anti)-collinear limit. In addition, the longitudinal momentum component ω for the light partonic constituent of the B -meson state can be defined by the kinematic relation $p_1 \cdot k = \bar{n} \cdot p_1 n \cdot k / 2 \equiv \bar{n} \cdot p_1 \omega / 2$ with the collinear- p_1 approximation, where the two light-cone vectors n_μ and \bar{n}_μ fulfill the constraints $n^2 = \bar{n}^2 = 0$ and $n \cdot \bar{n} = 2$. It is then convenient to simplify the quark/gluon propagators in the last line of (5) to

$$\frac{1}{y m_B^2 [\bar{x} - \omega/m_B + i\epsilon]} \frac{1}{y \bar{x} m_B^2 + i\epsilon}, \quad (6)$$

by applying the kinematic properties of $\bar{B}_q \rightarrow M_1 M_2$, the end-point behaviours of the twist-two distribution amplitudes for the final-state mesons [44, 45], and the momentum-fraction scaling rules of the Dirac trace in the second and third lines of (5).

We can readily verify that the obtained result (6) applies for both the generic $\bar{x} \sim \mathcal{O}(1)$ and the end-point region $\bar{x} \sim \mathcal{O}(\Lambda_{\text{QCD}}/m_B)$, which correspond to the anti-collinear and anti-soft-collinear [46, 47] momentum q_2 . This observation is in analogy

to the smooth interpolation of the A -type contribution to $\bar{B}_q \rightarrow \gamma \ell \bar{\ell}$ described by the SCET_I factorization formula (3.14) in [48]. In the anti-collinear q_2 case, the resulting convolution integrals in (5) become $\int_0^\infty d\omega \phi_B^+(\omega) \int_0^1 dx \int_0^1 dy \phi_{M_2}(x) \phi_{M_1}(y) / (\bar{x}^2 y)$ by dropping out the subleading term ω/m_B in (6), which reproduce exactly the obtained expression in [7] and develop the rapidity divergence thus spoiling the soft-collinear factorization at leading twist. The appearance of such singularity as $\bar{x} \rightarrow 0$ implies that both the hard and hard-collinear gluon exchanges (labelled with the red colour in Figure 1) will bring about the leading-power contribution to the flavour amplitude \mathcal{B}_1 , in spite of the phase-space suppression for the size of the hard-collinear region, which is compensated by the QCD enhancement from the hard-collinear quark and gluon propagators.

Having in mind the essential importance of including the hard and hard-collinear gluon exchange effects simultaneously, we proceed to write down the convolution integrals entering the factorized matrix element $\langle P_2^u \rangle_{(a)}^{(0)}$

$$\mathcal{G}_{\mathcal{B}_1} \equiv \int_0^\infty d\omega \phi_B^+(\omega) \int_0^1 dx \phi_{M_2}(x) \int_0^1 dy \phi_{M_1}(y) \\ \frac{1}{\bar{x} y (\bar{x} - \omega/m_B + i\epsilon)}, \quad (7)$$

which can be reduced to a rather compact form $\mathcal{G}_{\mathcal{B}_1} \approx 18 \left[\left(\ln \frac{m_B}{\lambda_B} + \gamma_E - 2 \right) - i\pi \right]$ in the leading-power approximation by employing the Grozin-Neubert model [42] for $\phi_B^+(\omega)$ and the asymptotic twist-two distribution amplitudes $\phi_{M_2}(x)$ and $\phi_{M_1}(y)$. The dimensionful quantity λ_B^{-1} represents the inverse moment of the above HQET distribution amplitude [40, 42, 49] and serves as an indispensable ingredient for the theory description of a wide variety of exclusive bottom-meson decays [48–58]. It is worthwhile to stress that we do not aim at implementing QCD resummation of the *perturbatively generated logarithms* of m_B/λ_B , which are nevertheless not numerically significant for the realistic \bar{B}_q -meson mass. The resulting factorization formula (7) provides a dynamical interpretation of the non-perturbative object X_A^i introduced in [7, 8] (with the superscript “ i ” characterizing the gluon emission from the initial-state quarks) with $X_A^i \approx \left[1 + \frac{(\gamma_E - 1) - i\pi}{\ln \frac{m_B}{\lambda_B}} \right] \ln \frac{m_B}{\lambda_B}$ explicitly, which can be matched onto the very parametrization $X_{A, \text{BBNS}}^i = (1 + \varrho_A e^{i\varphi_A}) \ln \frac{m_B}{\Lambda_h}$ suggested in [7, 8] by setting $\Lambda_h = \lambda_B$ and $(\varrho_A, \varphi_A) = \{(0.97, -97^\circ), (1.17, -97^\circ), (1.34, -97^\circ)\}$ for $\lambda_B = \{200, 350, 500\}$ MeV, respectively.

We are now ready to present the factorized expressions for the tree-level flavour amplitudes

$$\mathcal{B}_1 = \frac{1}{4} \left(C_2 - \frac{C_1}{2 N_c} \right) \hat{\mathcal{G}}_{\mathcal{B}_1}, \quad \mathcal{B}_4 = \frac{1}{8} \left[(C_4 + 16 C_6) \hat{\mathcal{G}}_{\mathcal{B}_1} + (C_4 + 4 C_6) \hat{\mathcal{G}}_{\mathcal{B}_4} \right], \quad \mathcal{B}_{4,\text{EW}} = \mathcal{B}_4 (C_4 \rightarrow C_{4Q}, C_6 \rightarrow C_{6Q}), \quad (8)$$

where $\widehat{\mathcal{G}}_{\mathcal{B}_1} = \mathcal{G}_{\mathcal{B}_1} + \int_0^1 dx \int_0^1 dy \phi_{M_2}(x) \phi_{M_1}(y)/(y(1-x\bar{y}))$ and $\widehat{\mathcal{G}}_{\mathcal{B}_4}$ can be obtained from $\widehat{\mathcal{G}}_{\mathcal{B}_1}$ by performing the replacement $x \leftrightarrow \bar{y}$ for the counterpart short-distance matching coefficient. Along the same vein we can derive the relevant results for the NLO topological amplitudes

$$\begin{aligned} \sum_{i=1}^6 C_i \mathcal{P}_i^{p,(1)} &= \left(C_2 - \frac{C_1}{2N_c} \right) H_1(m_p) + \left[(C_3 + 16C_5) - \frac{1}{2N_c} (C_4 + 16C_6) \right] [H_1(m_b) + H_1(0)] \\ &\quad + (C_4 + 10C_6) [H_1(m_b) + H_1(m_c) + 3H_1(0)] - \left[5C_4 - 8C_5 + 4 \left(\frac{1}{N_c} + 5 \right) C_6 \right] H_2, \\ C_8^{\text{eff}} \mathcal{P}_{8g}^{(1)} &= C_8^{\text{eff}} H_3, \quad \sum_{i=1}^6 C_i \mathcal{I}_i^{p,(1)} = [(C_3 + 4C_5) + C_F (C_4 + 4C_6)] H_4, \end{aligned} \quad (9)$$

where the explicit expressions of the H_i functions are presented in the Supplemental Material. In contrast to QCD factorization for the penguin contributions $H_{1,2,3}$, the one-loop building blocks $\mathcal{I}_i^{p,(1)}$ from the triangle diagram in Figure 1 (g) (plus the one with the two virtual gluons exchanged) are insensitive to the (anti)-hard-collinear dynamics at leading power, thus ensuring the disappearance of the HQET B -meson distribution amplitudes in the factorization formula for H_4 . Adopting the ansatz for the twist-two light-meson distribution amplitudes $\phi_{M_1}(x) = \phi_{M_2}(x)$, the peculiar linear combinations of Wilson coefficients C_i in the yielding result (9) for $\sum_{i=1}^6 C_i \mathcal{I}_i^{p,(1)}$ coincide with the emergent patterns for the annihilation-type contributions to the axial-vector form factors of $\bar{B}_q \rightarrow \gamma\ell\bar{\ell}, \gamma\gamma$ [48, 56]. This interesting observation, on the one hand, stems from the Bose-Einstein statistics for the transition matrix element

$$\begin{aligned} &\langle g^*(p_g, \alpha) g^*(\tilde{p}_g, \beta) | \mathcal{H}_{\text{eff}} | \bar{B}_q \rangle \\ &= i \epsilon_{\alpha\beta p_g \tilde{p}_g} F_V(p_g^2, \tilde{p}_g^2) + g_{\alpha\beta}^\perp F_A(p_g^2, \tilde{p}_g^2) \end{aligned} \quad (10)$$

with the two transversely polarized gluons, which leads to the form-factor relations $F_V(p_g^2, \tilde{p}_g^2) = -F_V(\tilde{p}_g^2, p_g^2)$ and $F_A(p_g^2, \tilde{p}_g^2) = F_A(\tilde{p}_g^2, p_g^2)$. On the other hand, this can be attributed to the symmetry constraints of the QCD matrix element

$$\begin{aligned} &\langle M_1(p) M_2(q) | g^*(p_g, \alpha) g^*(\tilde{p}_g, \beta) \rangle \\ &= \begin{cases} g_{\alpha\beta}^\perp \mathcal{S}_{\parallel}(M_1 M_2) & \text{for } M_1 M_2 = PP, V_L V_L, \\ i \epsilon_{\alpha\beta p_g \tilde{p}_g} \mathcal{S}_{\perp}(M_1 M_2) & \text{for } M_1 M_2 = PV, VP, \end{cases} \end{aligned} \quad (11)$$

which guarantee the transversity amplitudes $\mathcal{S}_{\parallel,\perp}$ proportional to the products of the twist-two distribution amplitudes $\phi_{M_2}(x) \phi_{M_1}(y)$. Combining together the requirements of the hadronic matrix elements (10) and (11) as discussed above, we are then led to conclude that only the axial-vector form factor F_A will be in demand when evaluating the NLO quantities displayed in (4). It is also apparent that the observed perturbative enhancement due to the penguin contractions of $P_{1,2}^c$ does not apply to the charmless $\bar{B}_q \rightarrow PV$ decays, which will therefore not be discussed in the subsequent numerical analysis.

PHENOMENOLOGICAL IMPLICATIONS

We are now equipped to explore the phenomenological significance of the factorized expressions for the hadronic quantities $\mathcal{T}^{p,(0)}$ and $\mathcal{T}^{p,(1)}$ dictating the exclusive $\bar{B}_q \rightarrow M_1 M_2$ decay amplitude (2). To this end, we will employ the three-parameter ansatz of the leading-twist bottom-meson distribution amplitude as proposed in [55] (see [59–68] for additional discussions on the higher-twist distribution amplitudes) $\phi_B^+(w, \mu_0) = \frac{\Gamma(\beta)}{\Gamma(\alpha)} U \left(\beta - \alpha, 3 - \alpha, \frac{w}{\omega_0} \right) \frac{w}{\omega_0^2} \exp \left(-\frac{w}{\omega_0} \right)$ at the reference scale $\mu_0 = 1 \text{ GeV}$, where $U(a, b, z)$ represents the confluent hypergeometric function of the second kind and the allowed intervals of the shape parameters ω_0 , α and β are determined by reproducing the numerical values of the inverse-logarithmic moments [48, 56] $\lambda_{B_d} = 350 \pm 150 \text{ MeV}$, $\lambda_{B_s} = 400 \pm 150 \text{ MeV}$, $\hat{\sigma}_{B_{d,s}}^{(1)} = 0.0 \pm 0.7$, $\hat{\sigma}_{B_{d,s}}^{(2)} = 0.0 \pm 6.0$. We proceed to adopt the lattice predictions for the pseudoscalar-meson decay constants (f_{B_d} , f_{B_s} , f_π , f_K) as summarized in [69] and take the improved extractions of the decay constants of the longitudinally polarized vector mesons (f_ρ , f_ω , f_ϕ) from [70]. Furthermore, we will truncate the Gegenbauer expansions of the twist-two light-meson distribution amplitudes at the next-to-next-to-leading conformal spin accuracy and take advantage of the non-perturbative determinations of the two lowest moments $a_{1,2}(\mu_0)$ from [71] for the energetic pseudoscalar mesons and from [70] for the light vector mesons. The default values and uncertainties for the remaining SM parameters follow Table 1 of [56].

In order to develop a transparent understanding of the numerical feature for the identified enhancement mechanism, we present in Table I the obtained results of $\mathcal{T}^{p,(0)}$ and $\mathcal{T}^{p,(1)}$ for the weak annihilation decay $\bar{B}_s \rightarrow \pi^+ \pi^-$ with three distinct values of the renormalization scale $\nu = m_b/2, m_b, 2m_b$, while employing the central values of the remaining theory inputs. Interestingly, the dominant NLO contribution from the charm-loop diagrams displayed in Figure 1 (c) and (d) (plus the two diagrams due to the crossing symmetry) will result in the signif-

	$\nu = m_b/2$	$\nu = m_b$	$\nu = 2m_b$
$\mathcal{T}^{u,(0)}$	$2.03 - 17.7i$	$2.00 - 17.4i$	$1.97 - 17.2i$
$\mathcal{T}^{c,(0)}$	$-0.38 + 3.35i$	$-0.25 + 2.16i$	$-0.16 + 1.42i$
$\alpha_s/(4\pi) \mathcal{T}^{u,(1)}$	$-2.29 - 3.63i$	$-2.41 - 3.61i$	$-2.47 - 3.57i$
$\alpha_s/(4\pi) \mathcal{T}^{c,(1)}$	$-1.65 - 2.34i$	$-1.82 - 2.40i$	$-1.91 - 2.43i$

TABLE I. Numerical predictions of the dynamical quantities $\mathcal{T}^{p,(0)}$ and $\mathcal{T}^{p,(1)}$ ($p = u, c$) for $\bar{B}_s \rightarrow \pi^+ \pi^-$ with three distinct renormalization scales ν .

	$\mathcal{A}_{\text{CP}}^{\text{dir}}$	$\mathcal{A}_{\text{CP}}^{\text{mix}}$
$\bar{B}_s \rightarrow \pi^+ \pi^-, \pi^0 \pi^0$	$-36.3_{-1.3}^{+8.2} (0.0 \pm 0.0)$	$-4.2_{-9.0}^{+21.4} (35.9_{-11.2}^{+15.6})$
$\bar{B}_s \rightarrow \rho_L^+ \rho_L^-, \rho_L^0 \rho_L^0$	$-36.3_{-1.8}^{+8.3} (0.0 \pm 0.0)$	$-4.3_{-9.0}^{+21.5} (35.9_{-11.2}^{+15.6})$
$\bar{B}_s \rightarrow \omega_L \omega_L$	$-36.3_{-3.1}^{+8.3} (0.0 \pm 0.0)$	$-3.8_{-9.7}^{+21.8} (35.9_{-11.2}^{+15.6})$
$\bar{B}_s \rightarrow \rho_L \omega_L$	$0.0 \pm 0.0 (0.0 \pm 0.0)$	$-71.0_{-5.4}^{+6.3} (-71.0_{-5.4}^{+6.3})$
$\bar{B}_d \rightarrow K^+ K^-$	$39.0_{-5.6}^{+3.2} (0.0 \pm 0.0)$	$-2.2_{-26.4}^{+19.1} (-47.0_{-18.8}^{+15.7})$
$\bar{B}_d \rightarrow K_L^{*+} K_L^{*-}$	$39.6_{-6.7}^{+4.9} (0.0 \pm 0.0)$	$-1.4_{-26.9}^{+19.7} (-47.0_{-18.8}^{+15.7})$
$\bar{B}_d \rightarrow \phi_L \phi_L$	$38.3_{-15.8}^{+11.4} (0.0 \pm 0.0)$	$27.8_{-25.9}^{+5.7} (0.0 \pm 0.0)$

TABLE II. Theory predictions of the CP asymmetries $\mathcal{A}_{\text{CP}}^{\text{dir}}$ and $\mathcal{A}_{\text{CP}}^{\text{mix}}$ (in units of 10^{-2}) for the weak annihilation $\bar{B}_q \rightarrow PP, V_L V_L$ decay processes, where we have included in parentheses the corresponding LO QCD results for a comparison.

ificant increase of the real part of $\mathcal{T}^{c,(0)}$ in magnitude and simultaneously generates the considerable cancellation of its imaginary part, keeping in mind the CKM hierarchy $V_{ub}V_{us}^*/V_{cb}V_{cs}^* = 0.021 e^{-1.20i}$. In consequence, the perturbative rescattering effect under discussion provides an important source of the strong phases of the weak-annihilation non-leptonic \bar{B}_q -meson decay amplitudes, which can then be probed feasibly by investigating the CP violating observables.

It is straightforward to derive the time-dependent CP asymmetries for the neutral \bar{B}_q -meson decaying into CP eigenstates

$$\begin{aligned} \mathcal{A}_{\text{CP}}(t) &= \frac{\Gamma(\bar{B}_q \rightarrow M_1 M_2) - \Gamma(\bar{B}_q \rightarrow M_1 M_2)}{\Gamma(\bar{B}_q \rightarrow M_1 M_2) + \Gamma(\bar{B}_q \rightarrow M_1 M_2)} \\ &= -\frac{\mathcal{A}_{\text{CP}}^{\text{dir}} \cos(\Delta m_q t) + \mathcal{A}_{\text{CP}}^{\text{mix}} \sin(\Delta m_q t)}{\cosh(\Delta \Gamma_q t/2) + \mathcal{A}_{\Delta \Gamma} \sinh(\Delta \Gamma_q t/2)}, \quad (12) \end{aligned}$$

where the general definitions of $\mathcal{A}_{\text{CP}}^{\text{dir}}$, $\mathcal{A}_{\text{CP}}^{\text{mix}}$ and $\mathcal{A}_{\Delta \Gamma}$ can be found, for instance, in [72–74], satisfying the exact algebra relation $|\mathcal{A}_{\text{CP}}^{\text{dir}}|^2 + |\mathcal{A}_{\text{CP}}^{\text{mix}}|^2 + |\mathcal{A}_{\Delta \Gamma}|^2 = 1$. The resulting predictions for the two independent CP asymmetries displayed in Table II evidently reveal the striking numerical impacts of the enhanced NLO QCD cor-

rection to the weak annihilation amplitudes described in this Letter, without which the direct CP violation for the entire pure annihilation channels would vanish due to the absence of at least two separate terms with different strong phases involved in $\bar{A}(\bar{B}_q \rightarrow M_1 M_2)$. By contrast, the time-dependent CP asymmetries of $\bar{B}_s \rightarrow \rho_L \omega_L$ turn out to be insensitive to this particular perturbative contribution in question, on account of the isospin non-conservation of the QCD scattering amplitude $\langle \rho_L(p) \omega_L(q) | g^*(p_g, \alpha) g^*(\tilde{p}_g, \beta) \rangle$. We further mention in passing that the newly computed NLO quantities $\mathcal{T}^{p,(1)}$ generate the subdominant corrections to the CP-averaged branching fractions of the pure annihilation decay channels (numerically at the level of $\mathcal{O}(10\%)$).

CONCLUSIONS

To summarize, we have endeavored to achieve the analytical regularization of end-point divergences in the factorization formulae of the peculiar weak annihilation non-leptonic bottom-meson decay amplitudes, due to the gluon radiation off the initial-state partons, by adding the missing hard-collinear contribution on top of the hard gluon exchange effect, both of which led to the leading power contributions in the heavy quark expansion. Applying the improved factorization formalism, we then identified the novel perturbative mechanism generated by the penguin contractions of the current-current operators, yielding the significant numerical impacts on the strong phases of the pure annihilation amplitudes. Our results are of importance for enhancing the predictive power of the perturbative factorization approach in addressing the entire spectrum of CP violating observables from exclusive heavy hadron decays, accessible at the LHCb and Belle II experiments.

ACKNOWLEDGEMENTS

We would like to thank Martin Beneke for interesting discussions and comments on the manuscript. The research of C.D.L. is supported by the National Natural Science Foundation of China with Grant No. 11521505 and 12070131001 as well as the National Key Research and Development Program of China under Contract No. 2020YFA0406400. C.W. is supported in part by the National Natural Science Foundation of China with Grant No. 12105112 and the Natural Science Foundation of Jiangsu Education Committee with Grant No. 21KJB140027. The research of Y.L.S. is supported by the National Natural Science Foundation of China with Grant No. 12175218 and the Natural Science Foundation of Shandong with Grant No. ZR2020MA093. Y.M.W. acknowledges support from the National Natural Science Foundation of China with Grant No. 11735010 and

12075125, and the Natural Science Foundation of Tianjin

with Grant No. 19JCJQJC61100.

Supplemental Material: Analytic Expressions for the NLO Kernels

We collect QCD factorization formulae for the primitive kernels entering the NLO topological amplitudes (9)

$$\begin{aligned} H_{i \leq 3} &= \frac{1}{12} \int_0^\infty d\omega \phi_B^+(\omega) \int_0^1 dx \phi_{M_2}(x) \int_0^1 dy \phi_{M_1}(y) \left[\left(\frac{h_i}{\bar{x}y} \left(\frac{1}{\bar{x} - \omega/m_B + i\epsilon} + \frac{\eta_i \bar{x}}{1 - x\bar{y}} \right) + \{x \leftrightarrow \bar{y}\} \right) + \{x \leftrightarrow y\} \right], \\ H_4 &= 2 \int_0^1 dx \phi_{M_2}(x) \int_0^1 dy \phi_{M_1}(y) \frac{1}{\lambda} \left[h_4 \frac{\bar{x} + y}{\bar{x}y} + \frac{1}{x\bar{x}} \left(\frac{\pi}{\sqrt{3}} - \frac{\lambda}{2y\bar{y}} \right) + \left(1 + \frac{\lambda}{4\bar{x}y} \left(2 + \frac{3}{x\bar{y}} \right) \right) \eta_4 + \{x \leftrightarrow y\} \right], \end{aligned} \quad (13)$$

where for brevity we have introduced the following perturbative functions

$$\begin{aligned} h_1 &= \ln \frac{m_q^2}{\mu^2} + \frac{1}{3} - \frac{4z_q}{x\bar{y}} + 2 \left(1 + \frac{2z_q}{x\bar{y}} \right) \sqrt{\frac{4z_q}{x\bar{y}} - 1} \arctan \frac{1}{\sqrt{\frac{4z_q}{x\bar{y}} - 1}}, \quad z_q = \frac{m_q^2}{m_B^2}, \\ h_2 &= 1, \quad h_3 = -\frac{3}{\bar{y}}, \quad h_4 = -2\sqrt{\frac{4}{x\bar{y}} - 1} \arctan \frac{1}{\sqrt{\frac{4}{x\bar{y}} - 1}}, \quad \eta_1 = \eta_2 = 1, \quad \eta_3 = -\frac{y}{\bar{x}}, \\ \eta_4 &= \frac{1}{\sqrt{\lambda}} \sum_{i=1}^3 \left[\text{Li}_2 \left(\frac{\beta_i - 1}{\alpha_i + \beta_i} \right) + \text{Li}_2 \left(-\frac{\beta_i - 1}{\alpha_i - \beta_i} \right) - \text{Li}_2 \left(\frac{\beta_i + 1}{\alpha_i + \beta_i} \right) - \text{Li}_2 \left(-\frac{\beta_i + 1}{\alpha_i - \beta_i} \right) \right], \end{aligned} \quad (14)$$

with the Källén function $\lambda \equiv \lambda(1, \bar{x}y, x\bar{y}) = (1 - x - y)^2$ and

$$\begin{aligned} \alpha_1 &= \sqrt{1 + \frac{4}{-\bar{x}y - i\epsilon}}, \quad \alpha_2 = \sqrt{1 + \frac{4}{-x\bar{y} - i\epsilon}}, \quad \alpha_3 = \sqrt{5}, \\ \beta_1 &= \frac{-\bar{x}y + x\bar{y} + 1}{\sqrt{\lambda}}, \quad \beta_2 = \frac{-x\bar{y} + 1 + \bar{x}y}{\sqrt{\lambda}}, \quad \beta_3 = \frac{-1 + x\bar{y} + \bar{x}y}{\sqrt{\lambda}}. \end{aligned} \quad (15)$$

* lucd@ihep.ac.cn

† corresponding author: shenylmeteor@ouc.edu.cn

‡ corresponding author: chaowang@nankai.edu.cn

§ corresponding author: wangyuming@nankai.edu.cn

- [1] M. Beneke, G. Buchalla, M. Neubert, and C. T. Sachrajda, Phys. Rev. Lett. **83**, 1914 (1999), arXiv:hep-ph/9905312.
- [2] M. Beneke, G. Buchalla, M. Neubert, and C. T. Sachrajda, Nucl. Phys. B **591**, 313 (2000), arXiv:hep-ph/0006124.
- [3] J. Chay and C. Kim, Nucl. Phys. B **680**, 302 (2004), arXiv:hep-ph/0301262.
- [4] M. Beneke, A. P. Chapovsky, M. Diehl, and T. Feldmann, Nucl. Phys. B **643**, 431 (2002), arXiv:hep-ph/0206152.
- [5] C. W. Bauer, D. Pirjol, I. Z. Rothstein, and I. W. Stewart, Phys. Rev. D **70**, 054015 (2004), arXiv:hep-ph/0401188.
- [6] C. W. Bauer, I. Z. Rothstein, and I. W. Stewart, Phys. Rev. D **74**, 034010 (2006), arXiv:hep-ph/0510241.
- [7] M. Beneke, G. Buchalla, M. Neubert, and C. T. Sachrajda, Nucl. Phys. B **606**, 245 (2001), arXiv:hep-

ph/0104110.

- [8] M. Beneke and M. Neubert, Nucl. Phys. B **675**, 333 (2003), arXiv:hep-ph/0308039.
- [9] M. Beneke, J. Rohrer, and D. Yang, Nucl. Phys. B **774**, 64 (2007), arXiv:hep-ph/0612290.
- [10] M. Bartsch, G. Buchalla, and C. Kraus, (2008), arXiv:0810.0249 [hep-ph].
- [11] H.-Y. Cheng and K.-C. Yang, Phys. Rev. D **78**, 094001 (2008), [Erratum: Phys. Rev. D **79**, 039903 (2009)], arXiv:0805.0329 [hep-ph].
- [12] H.-Y. Cheng and C.-K. Chua, Phys. Rev. D **80**, 114008 (2009), arXiv:0909.5229 [hep-ph].
- [13] H.-Y. Cheng and C.-K. Chua, Phys. Rev. D **80**, 114026 (2009), arXiv:0910.5237 [hep-ph].
- [14] G. Zhu, Phys. Lett. B **702**, 408 (2011), arXiv:1106.4709 [hep-ph].
- [15] K. Wang and G. Zhu, Phys. Rev. D **88**, 014043 (2013), arXiv:1304.7438 [hep-ph].
- [16] C. Bobeth, M. Gorbahn, and S. Vickers, Eur. Phys. J. C **75**, 340 (2015), arXiv:1409.3252 [hep-ph].
- [17] Q. Chang, J. Sun, Y. Yang, and X. Li, Phys. Lett. B **740**, 56 (2015), arXiv:1409.2995 [hep-ph].
- [18] Q. Chang, X.-N. Li, J.-F. Sun, and Y.-L. Yang, J. Phys. G **43**, 105004 (2016), arXiv:1610.02747 [hep-ph].

- [19] Q. Chang, X. Li, X.-Q. Li, and J. Sun, Eur. Phys. J. C **77**, 415 (2017), arXiv:1706.06138 [hep-ph].
- [20] C. M. Arnesen, Z. Ligeti, I. Z. Rothstein, and I. W. Stewart, Phys. Rev. D **77**, 054006 (2008), arXiv:hep-ph/0607001.
- [21] A. Khodjamirian, T. Mannel, M. Melcher, and B. Melic, Phys. Rev. D **72**, 094012 (2005), arXiv:hep-ph/0509049.
- [22] T. Feldmann and T. Hurth, JHEP **11**, 037 (2004), arXiv:hep-ph/0408188.
- [23] Y. Y. Keum, H.-N. Li, and A. I. Sanda, Phys. Rev. D **63**, 054008 (2001), arXiv:hep-ph/0004173.
- [24] C.-D. Lu, K. Ukai, and M.-Z. Yang, Phys. Rev. D **63**, 074009 (2001), arXiv:hep-ph/0004213.
- [25] Y. Li, C.-D. Lu, Z.-J. Xiao, and X.-Q. Yu, Phys. Rev. D **70**, 034009 (2004), arXiv:hep-ph/0404028.
- [26] A. Ali, G. Kramer, Y. Li, C.-D. Lu, Y.-L. Shen, W. Wang, and Y.-M. Wang, Phys. Rev. D **76**, 074018 (2007), arXiv:hep-ph/0703162.
- [27] H.-n. Li, Y.-L. Shen, Y.-M. Wang, and H. Zou, Phys. Rev. D **83**, 054029 (2011), arXiv:1012.4098 [hep-ph].
- [28] H.-n. Li, Y.-L. Shen, and Y.-M. Wang, Phys. Rev. D **85**, 074004 (2012), arXiv:1201.5066 [hep-ph].
- [29] H.-N. Li, Y.-L. Shen, and Y.-M. Wang, JHEP **02**, 008 (2013), arXiv:1210.2978 [hep-ph].
- [30] H.-N. Li, Y.-L. Shen, and Y.-M. Wang, JHEP **01**, 004 (2014), arXiv:1310.3672 [hep-ph].
- [31] H.-n. Li and Y.-M. Wang, JHEP **06**, 013 (2015), arXiv:1410.7274 [hep-ph].
- [32] W. Altmannshofer *et al.* (Belle-II), PTEP **2019**, 123C01 (2019), [Erratum: PTEP 2020, 029201 (2020)], arXiv:1808.10567 [hep-ex].
- [33] K. G. Chetyrkin, M. Misiak, and M. Munz, Phys. Lett. B **400**, 206 (1997), [Erratum: Phys.Lett.B 425, 414 (1998)], arXiv:hep-ph/9612313.
- [34] K. G. Chetyrkin, M. Misiak, and M. Munz, Nucl. Phys. B **520**, 279 (1998), arXiv:hep-ph/9711280.
- [35] C. Bobeth, M. Misiak, and J. Urban, Nucl. Phys. B **574**, 291 (2000), arXiv:hep-ph/9910220.
- [36] C. Bobeth, P. Gambino, M. Gorbahn, and U. Haisch, JHEP **04**, 071 (2004), arXiv:hep-ph/0312090.
- [37] T. Huber, E. Lunghi, M. Misiak, and D. Wyler, Nucl. Phys. B **740**, 105 (2006), arXiv:hep-ph/0512066.
- [38] M. Beneke, T. Feldmann, and D. Seidel, Nucl. Phys. B **612**, 25 (2001), arXiv:hep-ph/0106067.
- [39] V. L. Chernyak and A. R. Zhitnitsky, Nucl. Phys. B **201**, 492 (1982), [Erratum: Nucl.Phys.B 214, 547 (1983)].
- [40] M. Beneke and T. Feldmann, Nucl. Phys. B **592**, 3 (2001), arXiv:hep-ph/0008255.
- [41] M. Beneke, Nucl. Phys. B Proc. Suppl. **111**, 62 (2002), arXiv:hep-ph/0202056.
- [42] A. G. Grozin and M. Neubert, Phys. Rev. D **55**, 272 (1997), arXiv:hep-ph/9607366.
- [43] G. Bell, T. Feldmann, Y.-M. Wang, and M. W. Y. Yip, JHEP **11**, 191 (2013), arXiv:1308.6114 [hep-ph].
- [44] V. M. Braun and I. E. Filyanov, Z. Phys. C **48**, 239 (1990).
- [45] P. Ball, V. M. Braun, Y. Koike, and K. Tanaka, Nucl. Phys. B **529**, 323 (1998), arXiv:hep-ph/9802299.
- [46] T. Becher, R. J. Hill, and M. Neubert, Phys. Rev. D **69**, 054017 (2004), arXiv:hep-ph/0308122.
- [47] T. Becher, M. Neubert, L. Rothen, and D. Y. Shao, Phys. Rev. Lett. **116**, 192001 (2016), arXiv:1508.06645 [hep-ph].
- [48] M. Beneke, C. Bobeth, and Y.-M. Wang, JHEP **12**, 148 (2020), arXiv:2008.12494 [hep-ph].
- [49] G. P. Korchemsky, D. Pirjol, and T.-M. Yan, Phys. Rev. D **61**, 114510 (2000), arXiv:hep-ph/9911427.
- [50] S. Descotes-Genon and C. T. Sachrajda, Nucl. Phys. B **650**, 356 (2003), arXiv:hep-ph/0209216.
- [51] S. W. Bosch, R. J. Hill, B. O. Lange, and M. Neubert, Phys. Rev. D **67**, 094014 (2003), arXiv:hep-ph/0301123.
- [52] M. Beneke and J. Rohrwild, Eur. Phys. J. C **71**, 1818 (2011), arXiv:1110.3228 [hep-ph].
- [53] Y.-M. Wang, JHEP **09**, 159 (2016), arXiv:1606.03080 [hep-ph].
- [54] Y.-M. Wang and Y.-L. Shen, JHEP **05**, 184 (2018), arXiv:1803.06667 [hep-ph].
- [55] M. Beneke, V. M. Braun, Y. Ji, and Y.-B. Wei, JHEP **07**, 154 (2018), arXiv:1804.04962 [hep-ph].
- [56] Y.-L. Shen, Y.-M. Wang, and Y.-B. Wei, JHEP **12**, 169 (2020), arXiv:2009.02723 [hep-ph].
- [57] M. Beneke, P. Böer, P. Rigatos, and K. K. Vos, Eur. Phys. J. C **81**, 638 (2021), arXiv:2102.10060 [hep-ph].
- [58] C. Wang, Y.-M. Wang, and Y.-B. Wei, (2021), arXiv:2111.11811 [hep-ph].
- [59] H. Kawamura, J. Kodaira, C.-F. Qiao, and K. Tanaka, Phys. Lett. B **523**, 111 (2001), [Erratum: Phys.Lett.B 536, 344–344 (2002)], arXiv:hep-ph/0109181.
- [60] H. Kawamura, J. Kodaira, C.-F. Qiao, and K. Tanaka, Int. J. Mod. Phys. A **18**, 1433 (2003), arXiv:hep-ph/0112146.
- [61] T. Huang, C.-F. Qiao, and X.-G. Wu, Phys. Rev. D **73**, 074004 (2006), arXiv:hep-ph/0507270.
- [62] X.-G. Wu and T. Huang, Chin. Sci. Bull. **59**, 3801 (2014), arXiv:1312.1455 [hep-ph].
- [63] A. Khodjamirian, T. Mannel, A. A. Pivovarov, and Y. M. Wang, JHEP **09**, 089 (2010), arXiv:1006.4945 [hep-ph].
- [64] Y.-M. Wang, Y.-B. Wei, Y.-L. Shen, and C.-D. Lü, JHEP **06**, 062 (2017), arXiv:1701.06810 [hep-ph].
- [65] V. M. Braun, Y. Ji, and A. N. Manashov, JHEP **05**, 022 (2017), arXiv:1703.02446 [hep-ph].
- [66] C.-D. Lü, Y.-L. Shen, Y.-M. Wang, and Y.-B. Wei, JHEP **01**, 024 (2019), arXiv:1810.00819 [hep-ph].
- [67] J. Gao, C.-D. Lü, Y.-L. Shen, Y.-M. Wang, and Y.-B. Wei, Phys. Rev. D **101**, 074035 (2020), arXiv:1907.11092 [hep-ph].
- [68] J. Gao, T. Huber, Y. Ji, C. Wang, Y.-M. Wang, and Y.-B. Wei, (2021), arXiv:2112.12674 [hep-ph].
- [69] Y. Aoki *et al.*, (2021), arXiv:2111.09849 [hep-lat].
- [70] A. Bharucha, D. M. Straub, and R. Zwicky, JHEP **08**, 098 (2016), arXiv:1503.05534 [hep-ph].
- [71] G. S. Bali, V. M. Braun, S. Bürger, M. Göckeler, M. Gruber, F. Hutzler, P. Korcyl, A. Schäfer, A. Sternbeck, and P. Wein (RQCD), JHEP **08**, 065 (2019), [Addendum: JHEP 11, 037 (2020)], arXiv:1903.08038 [hep-lat].
- [72] P. A. Zyla *et al.* (Particle Data Group), PTEP **2020**, 083C01 (2020).
- [73] U. Nierste, in *Helmholz International Summer School on Heavy Quark Physics* (2009) pp. 1–38, arXiv:0904.1869 [hep-ph].
- [74] *B physics at the Tevatron: Run II and beyond* (2001) arXiv:hep-ph/0201071.